



Effects of geosynthetics on reduction of reflection cracking in asphalt overlays

Ali Khodaii^{a,*}, Shahab Fallah^b, Fereidoon Moghadas Nejad^c

^a Department of Civil Engineering, Amirkabir University of Technology, Tehran, Iran

^b Highway Division, Department of Civil Engineering, Amirkabir University of Technology, Tehran, Iran

^c Department of Civil Engineering, Amirkabir University of Technology, Tehran, Iran

ARTICLE INFO

Article history:

Received 14 September 2007

Received in revised form 17 March 2008

Accepted 4 May 2008

Available online 7 July 2008

Keywords:

Reflection cracking

Asphalt

Overlays

Deformation

Geosynthetics

ABSTRACT

An experimental program was conducted to determine the effects of geosynthetic reinforcement on mitigating reflection cracking in asphalt overlays. The objectives of this study were to assess the effects of geosynthetic inclusion and its position on the accumulation of permanent deformation. Geogrid position, type of existing pavement, temperature, and joint/crack opening were varied in 24 model specimens tested. Crack propagation under repeated loading was monitored. Results indicate a significant reduction in the rate of crack propagation in reinforced samples compared to unreinforced samples and type of old pavement (concrete or asphalt pavement), geogrid position and temperature affected the type of crack propagation in asphalt overlays. Placing the geogrid at a one-third depth of overlay thickness from the bottom provided the maximum service life.

© 2008 Elsevier Ltd. All rights reserved.

1. Introduction

1.1. Overview

One of the more serious problems associated with the use of thin overlays is reflective cracking. This phenomenon is commonly defined as the propagation of cracks due to the movement of the underlying pavement or base course into and through the new overlay as a result of load-induced and/or temperature-induced stresses (Cleveland et al., 2002).

Reflection cracking has two major driving forces:

1. *The external wheel load*: this contributes to high stress and strain levels in the overlay above the existing crack. The discontinuity in the existing pavement reduces the bending stiffness of the rehabilitated pavement section and creates a stress concentration. When conditions are such that the stress state exceeds the fracture resistance of the overlay, a reflective crack can be initiated and/or propagated. A combination of mode I (opening) and mode II (shearing) stress leads to crack propagation through the overlay (De Bondt, 1998).

2. *Daily temperature variations*: the contraction of the discontinuous underlying pavement leads to additional concentrated tensile stresses in the overlay above the existing crack or joint. This phenomenon is almost exclusively linked to the pure mode I crack opening mechanism (Kim and Buttlar, 2002).

Because a number of variables are involved in the nature of reflection cracking, no solution for the complete prevention of crack propagation has yet been suggested. Only retardation of crack progress is the best solution strategy adopted so far. Incorporation of geosynthetic materials in the design of paved and unpaved road systems has been shown to improve the performance and service life of pavements.

The major functions of geosynthetic materials are separation, reinforcement, filtration, drainage and acting as a liquid barrier. In providing reinforcement, the geosynthetic material structurally strengthens the pavement section by changing the response of the pavement to loading (Koerner, 2005). Geogrid reinforcement provided a more uniform load distribution and a deduction in the rut depth at the surface of the asphalt course (Wasage et al., 2004). Inclusion of a geosynthetic interlayer may enhance the resistance to reflection cracking either by a stress-relief or a reinforcement mechanism, or by a combination of both. The function of the stress-relief of paving fabric interlayer system is the absorption of stress due to movement in the old, cracked pavement. The fairly thick asphalt paving fabric layer absorbs some of this movement and therefore helps protect the ACC overlay above from stress related

* Corresponding author. Tel./fax: +982164543010.

E-mail addresses: khodaii@aut.ac.ir (A. Khodaii), shahab_fallah@aut.ac.ir (S. Fallah), Moghadas@aut.ac.ir (F. Moghadas Nejad).

cracking (Marienfeld and Guram, 1999). The mechanism of reinforcement can only occur if the geosynthetic has a higher modulus and sufficient cross-sectional area to substantially strengthen the overlay (Lytton, 1989).

1.2. Literature review

During the past decade or so, various researchers have proposed solutions to retard reflection cracking based on field, laboratory and numerical investigations (Jayawickrama and Lytton, 1987). The field performance of geogrid-reinforced overlays was varied because it depends on construction procedures, position of the geogrid, interfacial treatment between layers, and weather conditions (Kuo and Hsu, 2003).

Guo and Zhang (1993) studied geogrid-reinforced asphalt overlays in the field and found that a glass fiber grid placed at the bottom of the overlay was effective in limiting cracks near the interface and increased bending strength by 42% and fatigue life by 80%.

Kim et al. (1999) conducted a laboratory test to study mode I reflection cracking in asphalt overlays with a polymer-modified asphalt mixture and Glass Grid or polypropylene film. To simulate an asphalt pavement overlaid on top of a crack in a concrete pavement, an asphalt mixture specimen was placed on top of two discontinuous concrete blocks. The result showed that when modified asphalt mixture was reinforced with the glass grid at the bottom of the asphalt layer, its fatigue life increased by a factor of 16.7. Brown et al. (1989), Chang et al. (1998) and Sobhan et al. (2005) placed asphalt beam specimens on two pieces of plywood that had a 10 mm gap at the center to simulate an existing joint or crack underneath the overlay, with the whole system placed on a rubber base representing the soil foundation. Reddy et al. (1999) studied the propagation of reflection cracks by placing asphalt beam specimens on small concrete blocks (at different gap intervals) simulating the broken PCC resting on an elastic foundation prepared with compression springs. Goulias and Ishai (1999) used a wheel-tracking device to test an overlay with a pre-sawn crack or notch underneath the specimens. Also Komatsu et al. (1998) conducted a laboratory test using a wheel-tracking device to evaluate crack resistance of geogrid-reinforced overlays on existing asphalt pavements with a 10 mm crack.

The studies described below were based on finite element analyses to simulate crack propagation in asphalt overlays. The cracking mechanism and growth inspired plenty of studies in order to remedy the problem. Castell et al. (2000) predicted crack growth rate with maximum strains and found that bottom-up cracking is more likely to be found than top-down cracking. Thick overlays were once considered to prevent bottom-up reflective cracks. Yet, Uhlmeier et al. (2000) investigated thick overlays and found cracks starting at the surface and propagating down ward. Sha (1993) also noticed top-down reflection cracking happened for thick overlays according to field observation in China. Kuo and Hsu (2003) used the ABAQUS finite element program to model geogrid-reinforced asphalt overlays on the old PCC pavement with joints/cracks. Old pavement support was modeled with continuous springs as Winkler foundation. They concluded that placing the geogrid at one-third depth of asphalt overlay thickness from the bottom had the minimum tensile strain. After this position, placing the geogrid in the middle of the asphalt overlay was the best placement for reducing tensile stress above the geogrid compared with the specimens with the geogrid placed at the bottom of the overlay.

In the present study, a laboratory experiment program and detailed analysis were employed. The primary objectives of the experimental phase were as follows: (I) to study the effects of placement of the geosynthetic in the overlay under the condition of mode I (bending) on the growth and propagation of the reflection

crack at different temperatures and over different existing pavements (asphalt or concrete), (II) to quantify the effectiveness of geosynthetics in retarding reflection cracking in asphalt overlays with different gap openings in old pavements, (III) to study the effect of temperature and type of old pavements and geosynthetic position on the direction of crack propagation (bottom-up or top-down cracking) in asphalt overlays. In the course of the study, an experimental technique was developed for mode I fracture testing using a servo-hydraulic dynamic testing machine. This paper presents the methodology and some of the significant results obtained from the work.

2. Experimental program

2.1. Test setup

The current study evaluated different test configurations based on the Brown et al. (1989), Chang et al. (1998), Kim et al. (1999) and Sobhan et al. (2005) researches and developed a setup shown schematically in Fig. 1. It consists of the following major components representing a layered pavement structure: (a) an asphalt overlay $380 \text{ mm}^L \times 150 \text{ mm}^W \times 75 \text{ mm}^H$, which may be unreinforced or reinforced at any depth, (b) a block of asphalt or concrete, simulating discontinuous existing pavements (depth 100 mm) and (c) a resilient subgrade modeled with neoprene rubber with an elastic modulus of $11\,000 \text{ kN/m}^2$.

Simulated-repeated loading was applied to the specimens using a hydraulic dynamic loading frame. Cyclic square loads were applied to the top center of the beam through a circular loading plate (112 mm diameter) with a frequency of 10 Hz simulating high speed traffic. A maximum load of 6.79 kN was applied to the specimen to create 690 kN/m^2 or 100 psi pressure on top of the specimen to model a truck wheel load. A 0.196 kN (20 kg) minimum load was used to keep the loading plate in place during dynamic loading. A UTM servo-hydraulic machine with computerized test control and data acquisition system was used for conducting the experimental program. The specimens were tested at two temperatures: 20 and $60 \text{ }^\circ\text{C}$. Before the specimens were tested, they were kept in a temperature chamber at the desired temperature for 2 h. Table 1 shows the independent variables used in the study.

2.2. Materials used

The AC used in this study to represent the overlay and old pavement is made of coarse aggregate, and asphalt binder. The

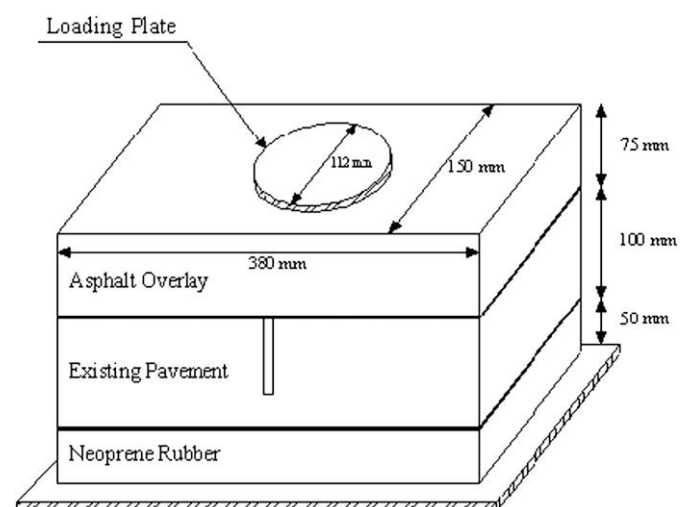


Fig. 1. Schematic of the test setup.

Table 1
Scope of experimental variables

Existing pavement	Width of crack/joint (mm)	Geogrid position ^a							
		None		Bottom		One-third		Middle	
		20 °C	60 °C	20 °C	60 °C	20 °C	60 °C	20 °C	60 °C
Concrete	10	✓	✓	✓	✓	✓	✓	✓	✓
	15	✓		✓		✓		✓	
	20	✓				✓			
Asphalt concrete	10	✓	✓	✓	✓	✓	✓	✓	✓
	15	✓		✓		✓		✓	
	20	✓				✓			

^a Distance from the bottom of the overlay.

grading of aggregate with the specification limits given by the *Iran Highway Asphalt Paving Code (2003)* is plotted in Fig. 2. Bitumen, AC 60-70 Penetration (that corresponds to PG 64-16), the most widely used in Iran, was used as binder for mixture preparation. The optimum asphalt binder content was 5.2% by weight of hot mix asphalt for each specimen.

The coarse aggregate used in the existing concrete pavement was natural gravel with a maximum size of 19 mm and a specific gravity of 2.58. The fine aggregate constituent was natural sand with a specific gravity of 2.54. The coarse and fine aggregate gradations met the BS 882 (BSI, 1973). The water to cement ratio was 0.52. The elastic modulus and compressive strengths for concrete specimens were 2.85×10^7 kN/m² and 343×10^2 kN/m², respectively.

2.3. Material and property of the grid

The geogrid used was one of the most frequently available and deployed in the country that was 100% polyester with a tensile strength of 50 kN/m at 12% strain in the machine direction and 14% strain in the cross machine direction and its mass per unit area was 240 g/m². The grid size was 40 mm × 40 mm.

2.4. Specimen preparation and placement configuration

To simulate an asphalt overlay on top of a crack in a concrete pavement, an asphalt mixture was designed using the Marshall procedure and placed on top of two discontinuous concrete blocks with a 100 mm height. The asphalt mixture specimen was bonded using a tack coat on top of the concrete block that had a 10 mm, 15 mm or 20 mm gap cut 2/3 the depth from the top. The crack or joint was made at the centerline of the old block using a water cooled circular saw with a diamond blade. For each asphalt overlay,

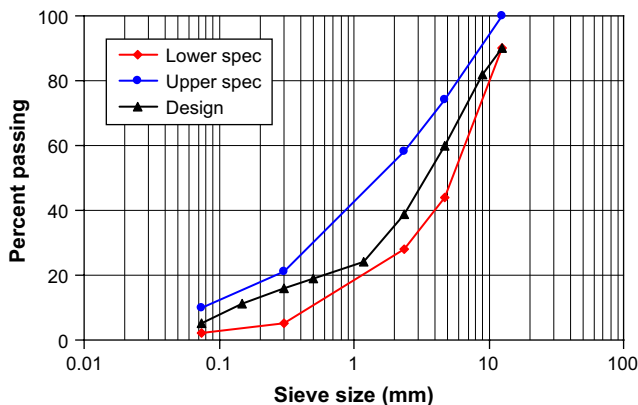


Fig. 2. Aggregate gradation used in asphalt concrete.

aggregate and binder were heated and mixed at a temperature of 150 °C. The amount of tack coat used between asphalt layer and concrete block was equal to 4.9×10^{-3} kN/m² and was of AC 85-100 penetration grade. The concrete block was placed in a steel mold with dimensions of 380 mm^L × 150 mm^W × 200 mm^H. A known weight of the hot mixture was poured on the concrete block in the steel mold in four layers. The hot mixture was compacted to a desired height using a hydraulic jack fitted with a flat steel plate 20 mm in thickness.

Table 2 shows the thickness and weight for each layer of overlay. Since the location of the geogrid for each type of specimen was different, these thicknesses were selected for all of the specimens in order to reach the same specific density.

The hot mixture was compacted to a desired height using a hydraulic jack fitted with a flat steel plate 20 mm in thickness. This procedure produced consistent specimens with the desired dimension and density. Specimens were prepared in four lifts at a target void content of 8.5% and weight of 2.123 kN/m³. Although the density of the compacted HMA specimen is slightly lower than the typical density used in the field, this density level was selected because it could be consistently achieved with the available hydraulic press in the laboratory. The following four types of specimens were prepared: (I) unreinforced specimens, which served as control specimens, (II) specimens with the geogrid placed on the concrete block, (III) specimens with the geogrid embedded at one-third depth of the asphalt concrete from the bottom. This was achieved by placing the geogrid on top of compacted first layer prior to pouring and compacting the loose mix of the next three layers, (IV) specimens with the geogrid embedded in the middle of the asphalt overlay, produced by placing the geogrid on top of the compacted second layer prior to pouring and compacting the loose mix of the next two layers. In two previous specimen preparations (III and IV), the reinforcement was sandwiched within the overlay.

The old asphalt concrete block was made from compacting of mixture in four layers in the steel mold (25 mm thickness for each layer). The characteristics of cracked asphalt were similar to the asphalt overlay. To simulate an asphalt overlay on top of the existing asphalt pavement with a crack, the preparation was the same as the asphalt overlay preparation on the concrete block with a joint/crack. Each specimen was then placed on the rubber foundation for testing with a hardness of Shore A=60 and Elastic Modulus of 11 000 kN/m² as shown in Fig. 3.

Two replicate specimens were fabricated and tested for each factor combination. A total of 48 specimens were tested.

Each experiment was recorded in its entirety by a video camera to allow the visual observation of reflection crack formation and propagation. Vertical crack growth was monitored with the camera and measured by processing of pictures every 600 cycles at 20 °C and 50 cycles at 60 °C from one side which was painted white with a water-based paint. The test was conducted until the vertical crack length reached the full specimen overlay depth (75 mm).

3. Result and analysis

Fig. 4 shows a typical failed, one-third embedded geosynthetic reinforced AC with a concrete block base that had a 10 mm crack/joint and unreinforced sample with an asphalt block base that had

Table 2
Thickness and weight for each layer of asphalt overlay

Layer number	Layer thickness (mm)	Weight (kg)
1	25.00	2.85
2	12.50	1.43
3	18.75	2.14
4	18.75	2.14



Fig. 3. Test specimen under load.

a 10 mm crack at different stages of failure. In the process of the test, crack initiation time (the time until small cracks are observed) and vertical crack propagation were recorded. Also vertical deformation was measured using the built in actuator of the UTM servo-hydraulic machine.

Dynamic stability, DS, was measured from the permanent deformation curves as described in Fig. 5. This value is the inverse of the rate of permanent deformation. Vertical crack growth rate was calculated from the slope of the linear regression line for each specimen and given in Table 3. The values in Table 3 are an average of the two specimens.

3.1. Effects of type of underlying pavement on optimum location of the geosynthetic

3.1.1. Effect of old concrete pavement

The crack propagations for specimens over existing concrete pavements were different depending on placement position of the geogrid in the overlay (at 20 °C). In the case of geogrids embedded at the bottom of the overlay, cracks occurred just over the joint. Then cracks developed under the loading continued to penetrate the entire layer and reached the top of the overlay. But in the case of the geogrid embedded in the middle or one-third depth, a top-down cracking pattern was identified. Immediately under the loading plate, cracks developed from the bottom of the lower layer of the AC overlay. Then the cracking energy was trapped by the geogrid. Finally, the upper layer of the AC overlay started to crack from top and propagated towards the geogrid. Placing the geogrid at one-third overlay thickness divides the overlay into a lower layer and an upper layer. This design is advantageous with the lower layer serving as a leveling layer that ensures good seating and bonding of the geogrid. In a theoretical simulation Brown et al. (2001) showed that placing a geosynthetic inside an asphalt overlay caused different stress distributions above and below the geosynthetic. Also Kuo and Hsu (2003) found that placing the geogrid at a one-third depth of the asphalt overlay thickness from the bottom had the minimum tensile strain above the geogrid and therefore had a maximum fatigue life compared with the

specimens with the geogrid placed at the bottom or in the middle of the asphalt overlay. They also noted that placing the geogrid inside the asphalt overlay distributes energy into two sub-layers.

Fig. 6 shows permanent deformation vs. load cycle and vertical crack growth vs. cycle for geogrid-reinforced and control samples without a geogrid with 10 mm gap in a concrete block. In general, fast vertical deformation occurs initially and then the slope of curves stabilizes. This is due to consolidation of mixtures at the initial stage of load application. It is observed that samples with reinforcement embedded at a one-third depth lasted longer than those embedded at the bottom. Dynamic stability (DS) of the unreinforced specimen was 28873 cycles/mm and that of the sample with a geogrid embedded at a one-third depth was 169926. This means that to create 1 mm of deflection, approximately 17×10^4 cycles of loading with 690 kN/m^2 (100 psi) pressure is required in specimens with the geogrid embedded at one-third depth. This number is approximately 5.9 times greater than that of the unreinforced specimen. The vertical crack growth rate of the unreinforced sample was the steepest ($30 \times 10^{-4} \text{ mm/cycles}$) of all samples. But vertical crack growth rate for samples with the geogrid was less than $14 \times 10^{-4} \text{ mm/cycle}$. The lowest crack growth rate was observed in the specimen with the geogrid embedded at one-third depth.

3.1.2. Effects of old asphalt concrete pavement

Crack propagation procedures for all of specimens with cracks in an old asphalt block base were the same. Cracks occurred first between the geogrid and overlay AC. Then cracks developed from the bottom of the overlay and propagated to the surface. Yet, the unreinforced specimen had wider cracks than reinforced specimens. The best location of the geogrid for reflection crack was found to be one-third depth from the bottom of the overlay that had a fatigue life 6.7 times greater than the unreinforced specimen. Also vertical crack growth rate for unreinforced sample was $15 \times 10^{-4} \text{ mm/cycles}$. The lowest rate was observed with reinforcement at one-third depth with a value of $2 \times 10^{-4} \text{ mm/cycle}$ as shown in Fig. 7 and Table 3. This means that 7.5 times as many load applications are required for cracks in the reinforced overlay with the geogrid at a one-third depth to grow the same length as that in the unreinforced specimen. Sobhan et al.'s (2005) studies showed that if the geosynthetic is embedded at the middle of the overlay it will provide a fatigue life greater than embedded in the bottom. It should be noted that they did not make a reinforced specimen at a one-third depth from the bottom.

Vertical crack growths for these specimens were slower than the samples with concrete blocks. But in these samples crack widths especially on the crack tip were bigger than specimens with concrete blocks. It is observed that samples with reinforcement embedded in the middle and one-third depth of the overlay lasted longer than when embedded at the bottom while accumulating less permanent deformation.

3.2. The effect of width of a joint/crack in old pavements in geogrid application

Because the best location for a geosynthetic in an overlay with old asphalt or concrete block that had a 10 mm gap interval was one-third depth from the bottom of the overlay, the other reinforced samples with reinforcement at a one-third depth with different gap intervals were made to compare with unreinforced samples with different gaps in the block. Three crack/joint widths were selected, 10 mm to simulate cracks developed in asphalt pavements and 15 or 20 mm to simulate a joint opening in an existing concrete pavement to be overlaid by asphaltic mixes.

By increasing the concrete block gap, crack propagation was faster than the sample with a 10 mm joint/crack. As shown in Fig. 8

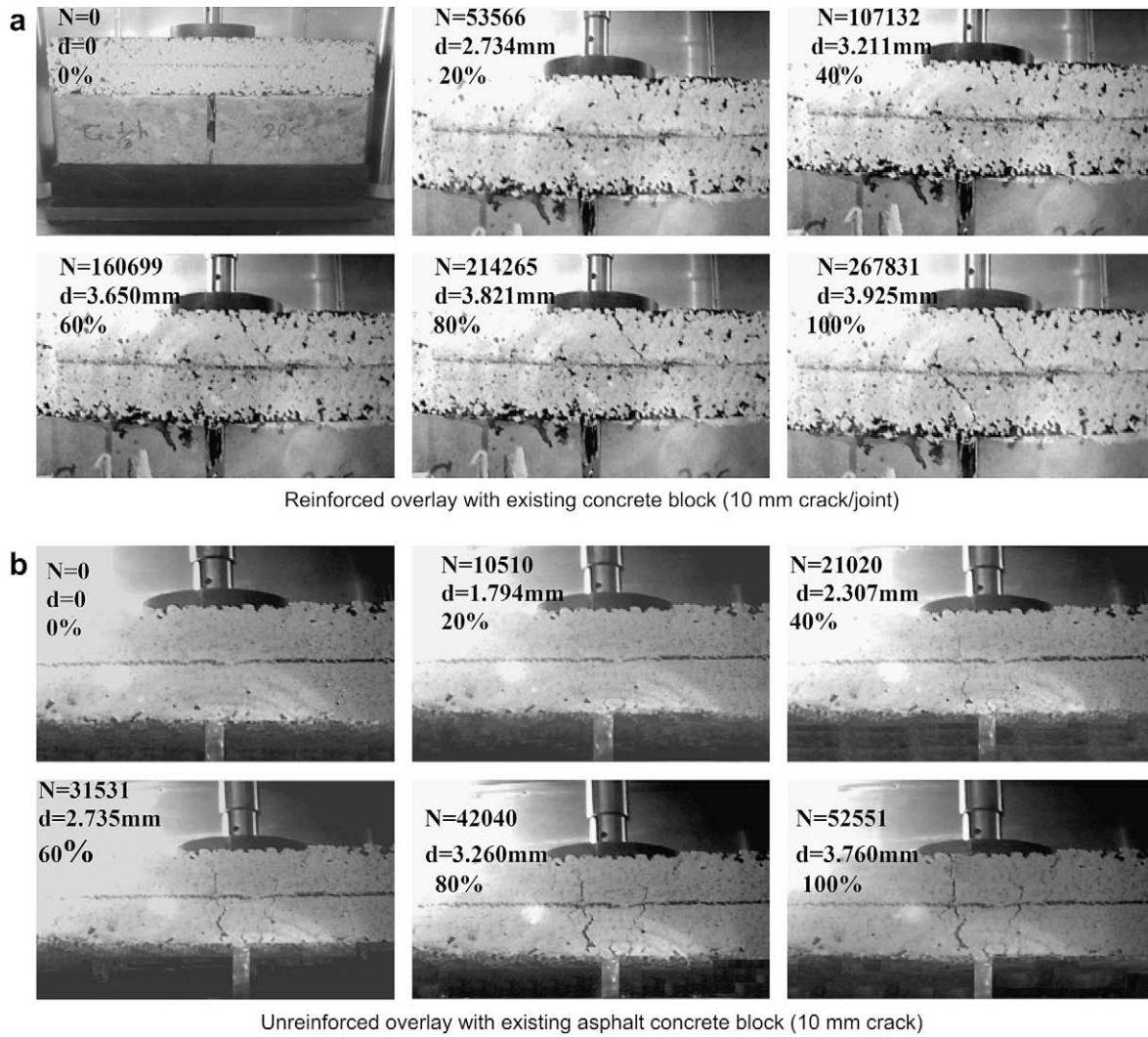


Fig. 4. Progression of reflection cracks at 20 °C for (a) geogrid reinforced (embedded at one-third) overlay and (b) unreinforced overlay. Note: N= the number of cycle and d= deflection at this cycle and 0%, 20%, 40%, 60%, 80% 100% corresponds the fatigue life percents.

and Table 3, reinforced overlay on concrete block with a 20 mm gap interval had 66% of fatigue life of a reinforced overlay on PCC with a 10 mm joint/crack. However, a specimen with the geogrid embedded at one-third depth of the overlay over a concrete block with 20 mm joint had a service life and crack initiation time 8.7 and 4.25 times that of the unreinforced specimen with a 20 mm gap, respectively.

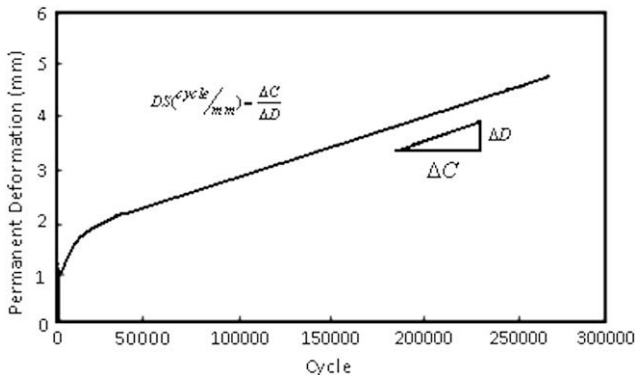


Fig. 5. Description of dynamic stability.

Also samples over an asphalt block base with a 15–20 mm gap had a greater crack growth rate and lower dynamic stability when compared with those placed over a 10 mm gap asphalt block base (Fig. 9).

The results in general indicate that the effect of reinforcing geogrids in overlays with an increasing joint/crack in existing pavements was almost constant.

3.3. Effects of high temperature

The reason for selecting this temperature (60 °C) is to recognize whether or not high temperature causes debonding between the geogrid and asphalt concrete under cyclic loading. Also, whether or not at high temperature a reinforced overlay had more service life than an unreinforced overlay.

At this temperature, all of the reinforced overlay with a concrete block base had a crack growth trend from top to bottom of the overlay. This phenomenon was similar to Kuo and Hsu's (2003) findings. But in specimens with asphalt concrete blocks, crack propagations were different. At 60 °C crack propagation for the reinforced overlay in the middle with existing asphalt pavements was top-down cracking. Although the modulus of the overlay and existing pavement was the same, the high temperature caused top-down cracking to happen in this specimen. The

Table 3
Mode I reflection crack propagation test results

Existing pavement	Test temperature (°C)	Width of joint/crack (mm)	Geogrid position	Service life (cycles)	Vertical displacement (mm)	Crack initiation (cycles)	Vertical DS (cycles/mm)	Vertical crack growth rate (mm/cycle × 10 ⁻⁴)
Concrete	20	10	None	31 551	2.796	6310	28 873	30
	20	10	Bottom	64 311	3.492	11 200	38 597	14
	20	10	One-third	254 653	3.811	38 400	169 926	3
	20	10	Middle	216 732	4.144	33 800	93 180	4
	20	15	None	27 831	3.028	4200	22 122	32
	20	15	One-third	193 911	3.914	15 600	113 265	4
	20	20	None	19 311	3.882	2400	10 706	44
	20	20	One-third	168 782	3.911	10 200	146 475	5
	60	10	None	1213	3.998	200	448	749
	60	10	Bottom	1865	5.223	250	541	488
	60	10	One-third	2810	6.544	450	527	269
	60	10	Middle	2701	7.230	400	554	288
	Asphalt concrete	20	10	None	52 551	3.761	4200	21 325
0		10	Bottom	153 211	5.443	9000	48 557	6
20		10	One-third	354 942	5.201	19 800	293 773	2
20		10	Middle	267 302	6.020	10 200	198 377	3
20		15	None	39 567	5.286	3600	10 653	20
20		15	One-third	231 540	6.691	16 200	67 603	4
20		20	None	20 031	6.239	2400	5232	41
20		20	One-third	127 810	8.449	13 800	23 453	7
60		10	None	1181	11.526	200	113	740
260		10	Bottom	1961	15.897	250	145	426
60		10	One-third	2381	14.957	400	204	377
60		10	Middle	2161	14.017	350	204	337

other three specimens had a crack growth from the bottom to the surface of the overlay (similar to all specimens at 20 °C). Because of high temperature and similarity in the overlay and base material, the permanent deformations of these samples were very high.

As shown in Figs. 10 and 11, specimens with the geogrid embedded at a one-third depth of the overlay had a maximum

service life (approximately two times greater than unreinforced) and had the lowest slope of vertical crack growth rate between all specimens. At this temperature, the effect of the geogrid located at a one-third depth of the overlay on reinforcing was approximately 30% of the same condition at 20 °C.

Service life for all various conditions is shown in Fig. 12. From this figure, the most and least effective geogrid position in the

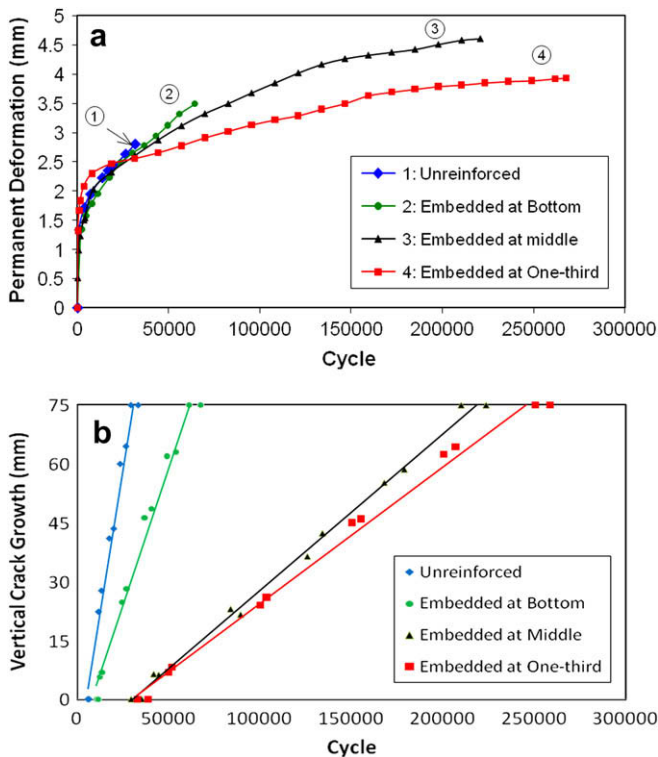


Fig. 6. Permanent deformation (a) and vertical crack growth rate (b) for overlays with a concrete block base and a 10 mm gap at 20 °C.

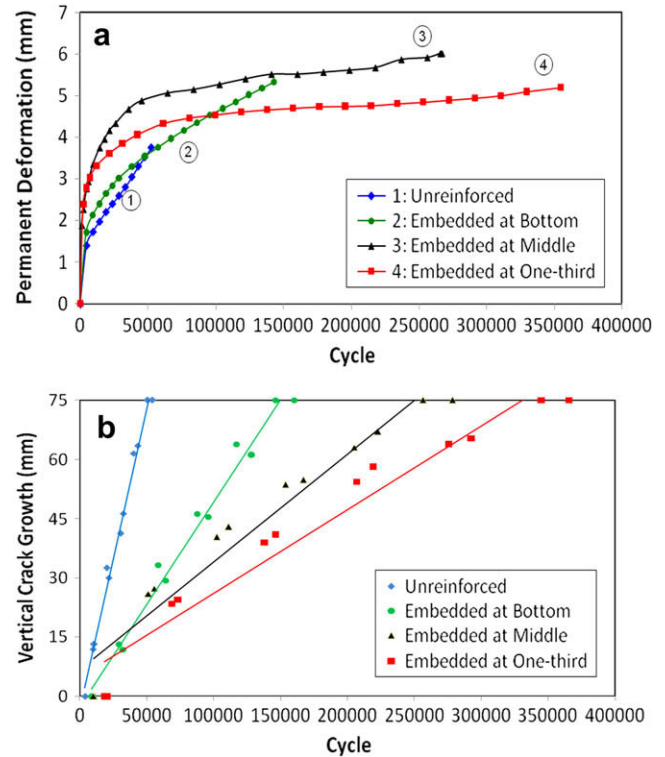


Fig. 7. Permanent deformation (a) and vertical crack growth rate (b) for overlays with an asphalt block base and 10 mm gap at 20 °C.

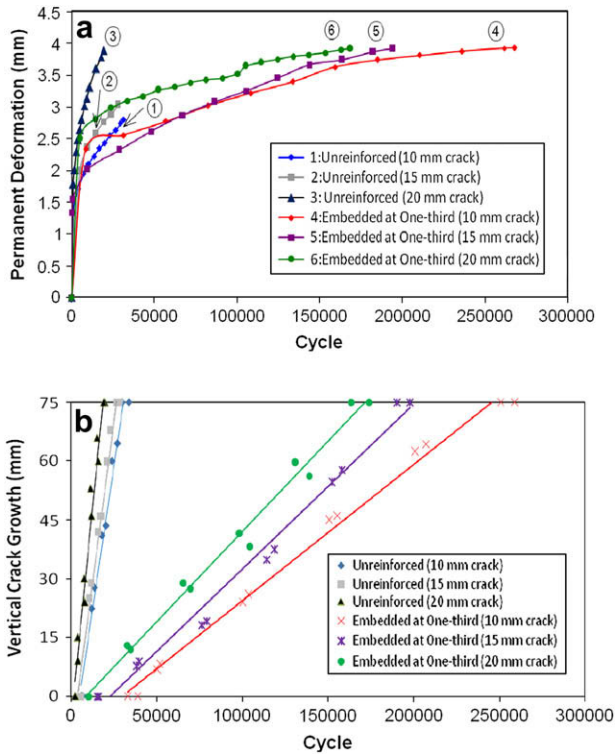


Fig. 8. Permanent deformation (a) and vertical crack growth rate (b) for unreinforced and reinforced overlays at a one-third depth with a concrete block base at 20 °C.

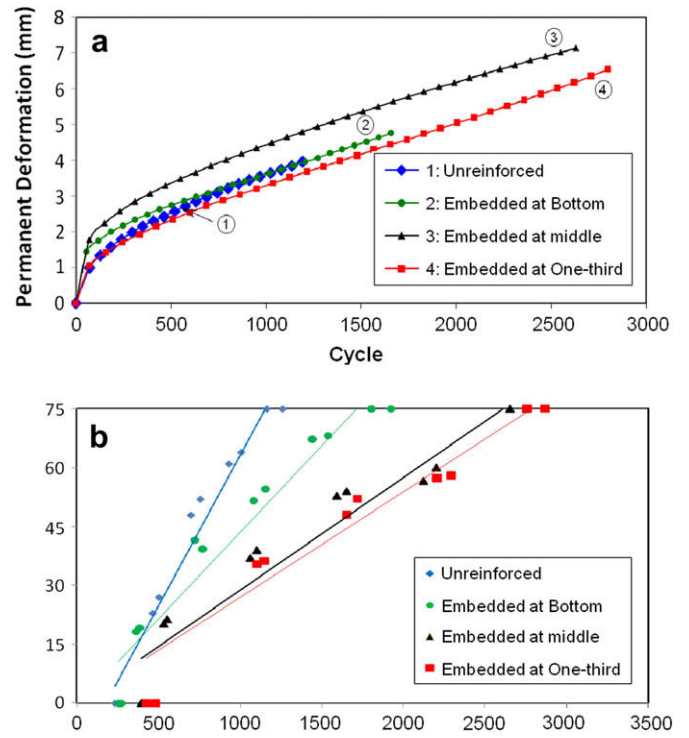


Fig. 10. Permanent deformation (a) and vertical crack growth rate (b) for overlays with a concrete block base and 10 mm gap at 60 °C.

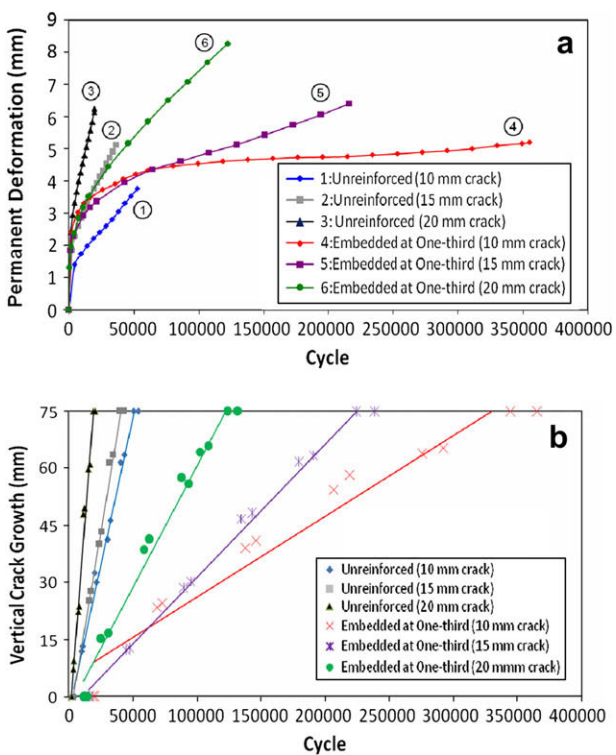


Fig. 9. Permanent deformation (a) and vertical crack growth rate (b) for unreinforced and reinforced overlays at a one-third depth with an asphalt block base at 20 °C.

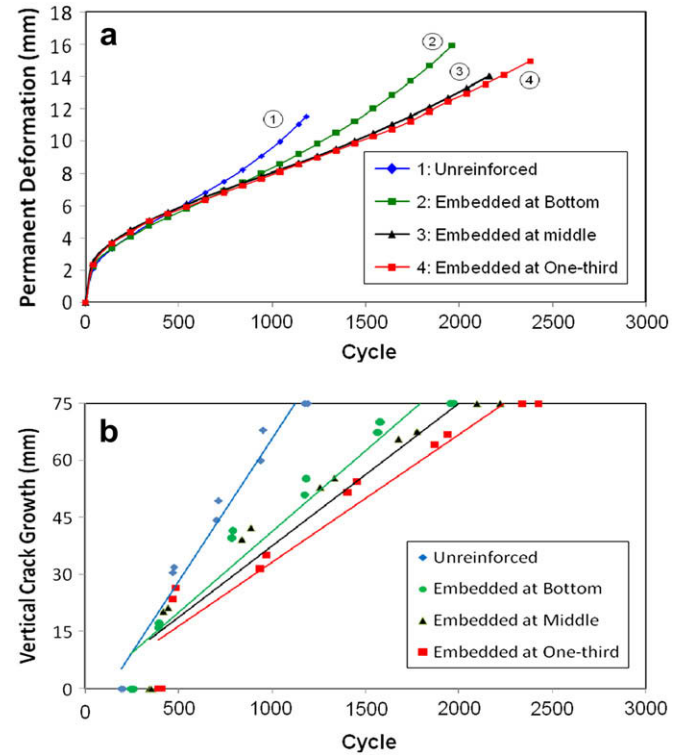


Fig. 11. Permanent deformation (a) and vertical crack growth rate (b) for overlays with an asphalt block base and 10 mm gap at 60 °C.

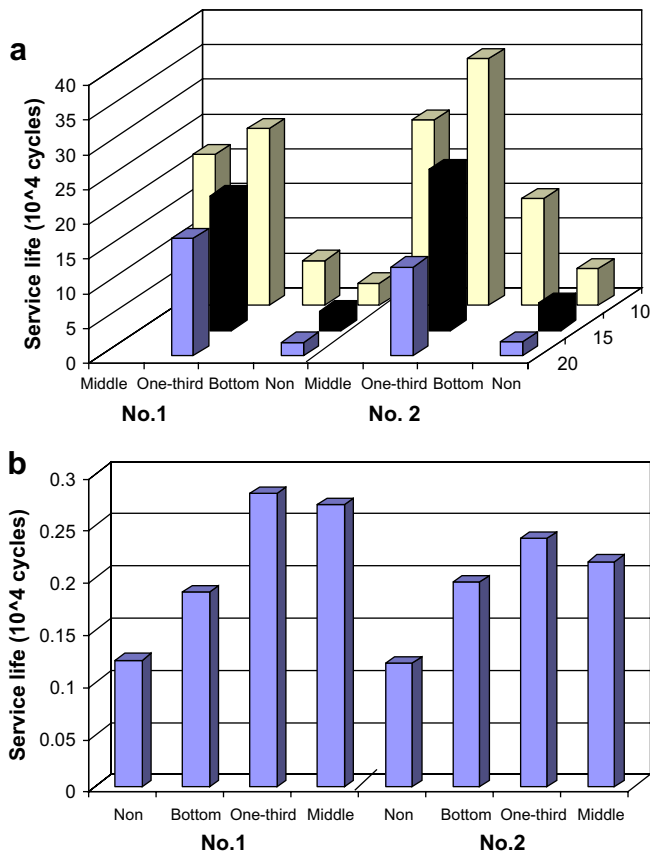


Fig. 12. Comparison of service life for various conditions: (a) fatigue life at 20 °C, (b) fatigue life at 60 °C.

Note: No. 1 and No. 2 represents overlay with old concrete block and asphalt concrete block respectively, 10, 15 and 20 corresponds to the width of crack in old block in mm.

asphalt overlay in relation to resistance to reflection cracking can be easily distinguished.

4. Conclusions

Data collected from these experiments verify that geogrid inclusion in the asphalt sample leads to a significant increase in overlay performance. Specimens with embedded geogrids outperformed non-reinforced samples both in terms of resistance to cracking as well as rutting. Although placing the geogrid at one-third depth forces the contractors to pour the overlay in two separate layers and hence encounters some extra cost, this position is most effective in retarding reflection cracking. This phenomenon is independent of type of old pavement and temperature. This design is advantageous with the lower layer serving as a leveling layer that ensures good seating and bonding of the geosynthetic.

The effect of the geogrid for overlay reinforcing with increasing crack/joint from 10 to 20 mm in existing pavements was not decreased. But at high temperature the effect of the geogrid in overlay reinforcing in proportions to low temperature was reduced.

According to the results section, the top-down cracking pattern in overlays depends on:

1. Geogrid position in the asphalt overlay.
2. Relative stiffness of the overlay to old pavement.
3. Temperature.

Future tests should focus on thermal cracking on reinforced specimens with different geogrid positions in the overlay to study

the effect of subsequent shrinkage and expansion of old concrete pavements at the bottom of overlays for optimizing the placement of geosynthetics in overlays.

Acknowledgement

We gratefully acknowledge the financial support from the Road Maintenance and Transportation Organization of Iran.

References

- British Standards Institution, 1973. BS 882: Part 2: 1973, Coarse and Fine Aggregates from Natural Sources. BSI, London.
- Brown, S.F., Brunton, J.M., and Armitage, R.J., 1989. Grid reinforced overlays, reflective cracking in pavements: assessment and control. Proceedings of the RILEM Conference, Liege, Belgium, March 8–10, pp. 63–70.
- Brown S.F., Thom N.H., Sanders P.J. 2001. A study of grid reinforced asphalt to combat reflection cracking. Annual Meeting of Association of Asphalt Paving Technologists, pp. 543–569.
- Castell, M.A., Ingrassia, A.R., Irwin, L.H., 2000. Fatigue crack growth in pavements. Journal of Transportation Engineering (ASCE) 126 (4), 283–290.
- Chang, D.T.T., Lai, R.Q., Chang, J.-Y., Wang, Y.-H., 1998. Effects of Geogrid in Enhancing the Resistance of Asphalt Concrete to Reflection Cracks. ASTM STP 1348. American Society for Testing and Materials, pp. 39–51.
- Cleveland, G.S., Button, J.W., Lytton, R.L., 2002. Geosynthetics in Flexible and Rigid Pavement Overlay Systems to Reduce Reflection Cracking. Report no. FHWA/TX-02/1777. Texas Department of Transportation Research and Technology Implementation Office, pp. 1–297.
- De Bondt, A.H., 1998. Anti-Reflective Cracking Design of (Reinforced) Asphalt Overlays. Ph.D. Thesis. Department of Civil Engineering, Delft University of Technology, Delft, The Netherlands.
- Goulias, D.G., Ishaq, I., 1999. Experimental system for simulating crack propagation in asphalt pavements and effectiveness of geosynthetics in crack retardation. Journal of Testing and Evaluation (ASTM) 27 (2), 106–113.
- Guo, Z., Zhang, Q., 1993. Prevention of cracking progress of asphalt overlay with glass fabric. Reflective cracking in pavements: state of the art and design recommendations. Proceedings of the Second International RILEM Conference, Liege, Belgium, 10–12, pp. 398–405.
- Iran Highway Asphalt Paving Code, 2003. Ministry of Road and Transportation Research and Education Center, Iran. No. 234.
- Jayawickrama, P.W., Lytton, R.L., 1987. Methodology for predicting asphalt concrete overlay life against reflective cracking. Proceedings of 6th International Conference on the Structural Design of Asphalt Pavements, vol. 1.
- Kim, J., Buttler, W.G., 2002. Analysis of reflective crack control system involving reinforcing grid over based-isolating interlayer mixture. Journal of Transportation Engineering (ASCE) 128 (4), 375–384.
- Kim, K.W., Doh, Y.S., Lim, S., 1999. Mode I reflection cracking resistance of strengthened asphalt concrete. Journal of Construction and Building Materials 13, 243–251.
- Koerner, R., 2005. Designing with Geosynthetic, fifth ed. Prentice Hall, Upper Saddle, New Jersey.
- Komatsu, T., Kikuta, H., Tuji, Y., Muramatsu, E., 1998. Durability assessment of geogrid-reinforced asphalt concrete. Journal of Geotextile and Geomembranes 16, 257–271.
- Kuo Ch.M., Hsu T.R., 2003. Traffic induced reflective cracking on pavements with geogrid reinforced asphalt concrete overlay. 82nd Annual TRB Meeting, pp. 1–23.
- Lytton, R.L., 1989. Use of geotextile for reinforcement and strain relief in asphalt concrete. Journal of Geotextile and Geomembranes 8, 217–237.
- Marienfild, M.L., Guram, S.K., 1999. Overview of field installation procedures for paving fabric in North America. Geotextile and Geomembranes 17, 105–120.
- Reddy S.K., Reddy R.K., Pandey B.B., 1999. Cracking in bituminous layers placed over cracked pavements. Presented at the 78th Annual Meeting of the Transportation Research Board, January, Washington, D.C.
- Sha, Q.L., 1993. Two kinds of mechanism of reflective cracking, reflective cracking in pavements: state of the art and design recommendations: Proceedings of the Second International RILEM Conference, Liege, Belgium.
- Sobhan, K., Genduso, M., Tandon, V., 2005. Effects of geosynthetic reinforcement on the propagation of reflection cracking and accumulation of permanent deformation in asphalt overlays. Third LACCET International Latin American and Caribbean Conference for Engineering and Technology (LACCET 2005) Advances in Engineering and Technology: A Global Perspective 8–10 June 2005, Cartagena, Columbia, pp. 1–9.
- Uhlmeier J.S., Pierce L.M., Willoughby K., Mahoney J.P., 2000. Top-down cracking in Washington state asphalt concrete wearing courses, Presented in the 79th Annual Meeting of Transportation Research Board, Washington D.C.
- Wasage, T.L.J., Ong, G.P., Fwa, T.F., Tan, S.A., 2004. Laboratory evaluation of rutting resistance of geosynthetics reinforced asphalt pavement. Journal of the Institution of Engineers Vol. 44 (2), 29–44.